J Clust Sci (2016) 27:421–429
DOI 10.1007/s10876-016-0968-0

BRIEF COMMUNICATION

A Green Approach for the Synthesis of Silver Nanoparticles Using Root Extract of *Chelidonium majus:* Characterization and Antibacterial Evaluation

Hossein Alishah[1] · Shahram Pour Seyedi[1] · S. Yousef Ebrahimipour[2] · Saeed Esmaeili-Mahani[3]

Received: 23 November 2015 / Published online: 25 January 2016

Abstract In this study, silver nanoparticles (Ag-NPs) have been synthesized using extract of *Chelidonium majus* root in aqueous solution at room temperature. The root extract was able to reduce Ag^{+} to Ag^{0} and stabilized the nanoparticles Different physico-chemical techniques including UV–Vis spectroscopy, transmission electron microscopy and powder X-ray diffraction (PXRD) were used for the characterization of the biosynthesized Ag-NPs obtained. The surface plasmon resonance band appeared at 431 nm is an evidence for formation of Ag-NPs. TEM imaging revealed that the synthesized Ag-NPs have an average diameter of around 15 nm and with spherical shape. Moreover the crystalline structure of synthesized nanoparticles was confirmed using XRD pattern. Furthermore antimicrobial activities of synthesized Ag-NPs were evaluated against *Escherichia coli* -ATCC 25922 and *Pseudomonas aeruginosa* ATCC 2785 bacteria strain.

Keywords Ag-NPs · XRD · TEM · Antimicrobial activity · *Chelidonium majus* · Green synthesis

✉ S. Yousef Ebrahimipour
ebrahimipour@ymail.com; ebrahimipour@uk.ac.ir

[1] Department of Biotechnology, Faculty of Agriculture, Shahid Bahonar University of Kerman, Kerman, Iran

[2] Department of Chemistry, Faculty of Science, Shahid Bahonar University of Kerman, Kerman, Iran

[3] Department of Biology, Faculty of Science, Shahid Bahonar University of Kerman, Kerman, Iran

Introduction

In recent years, nanotechnology has attracted more attention in science due to its different applications [1]. Size- and shape-dependent optical, electrical and electronic properties of nano-materials make them effectively applicable in different branches of science and technology [2, 3]. Among them, metal nanoparticles have attracted considerable attention due to their unique properties compared to bulk mater [4]. Potential applications of silver nanoparticles (Ag-NPs) in different fields have introduced these particles as one of the most important commercialized NPs [5]. Ag-NPs have been used extensively in industrial and medicinal fields [6]. Imaging, water and air purification, cosmetics, household appliances, textiles, energy sector, antibacterial and anticancer agents are the some important applications of Ag-NPs [5, 7–9].

Various techniques including wet chemical reduction [10], photochemical reduction [11], electrochemistry [12], X-ray [13], and UV irradiation [14], ultrasound assisted [15], microwave [16], and laser ablation [17] have been reported for the synthesis of Ag-NPs. Recently, biosynthesis of Ag-NPs using bio-reducing and bio-stabilizing agents produced by different biological systems such as bacteria, fungi, yeasts, algae or plants [18, 19] has received increasing attention due to its environmentally benign nature. However, the exact mechanism of biological reduction of Ag(I) to Ag is not completely understood. The ability of plant extracts to reduce metal ions to nanoparticles has been widely used for the synthesis of Ag-NPs because of its cost-effectiveness, simplicity and inherent safety [4, 20, 21].

Extracts of *Cinnamomum camphora* [22], *Ficus benghalensis* leaves [23], *Geranium* (*Pelargonium graveolense*) leaves [24], *Desmodium trifolium* [25] and *Datura metel* leaves [26] are some examples of plant materials used for the biosynthesis of Ag-NPs. In these cases, the extract is mixed with silver salt solution at room temperature. After a few minutes, the reduction reaction is completed. While in chemical synthesis, a reducing agent such as $NaBH_4$ and a stabilizing or capping agent such as polyvinyl alcohol are added to the silver salt for reducing the silver ions and controlling the growth, size and aggregating of the synthesized NPs, respectively [27]. Interestingly, the plant extracts used for the biosynthesis of Ag-NPs contain both required agents.

Herein, the extract of *Chelidonium majus* roots has been prepared and used for the green biosynthesis of Ag-NPs. The obtained NPs have been characterized with spectroscopy and imaging techniques. Additionally, the antibacterial activity of the Ag-NPs synthesized has been investigated.

Experimental

Materials and Instruments

$AgNO_3$ was purchased from Merck. Roots of *Chelidonium majus* were collected from Kerman, Iran. Deionized water was used in all experiments. All of the reagents

and solvents were procured from sigma. UV–Vis spectrophotometer (scan drop 250-211Fo75) was supplied from Analytic Jena (Germany). Transmission electron microscope (TEM) images were obtained using LEO912-AB, LEO Company. The XRD patterns of Ag-NPs were obtained using X-ray diffractometer (X PERTPRO, PANalitical, Germany) equipped Cu Ka (l = 1.54056 Å) radiation source in the range of 35°–80°, operating at 40 kV and 40 mA.

Synthesis of Nanoparticles

Roots of *Chelidonium majus* were washed with deionized water, and then dried at a given temperature for a week. To prepare an extract suitable for the synthesis of the NPs, 5 g of the roots was powdered and added to 100 ml deionized water. This mixture was kept under vigorous stirring at 100 °C for 30 min and then centrifuged twice at 4500 rpm for 20 min. The obtained extract was filtered through a Whatman-40 filter paper. A clear light-brown extract was resulted which were stored in refrigerator at 4 °C. For the synthesis of Ag NPs, 50 ml of the extract was added to 100 ml aqueous solution containing 3.5 mM of $AgNO_3$. After a few minutes, the NPs were synthesized which were stable for a long time. The obtained NPs solution was then stored at 28 °C for next experiments.

Antibacterial Activity

Antimicrobial activity of the Ag-NPs at the concentrations of 150 and 300 ppm was investigated against one type of *E-coli* which was isolated from some patients stricken with urinary tract infection (UTI), and two standard strains namely *E. coli*-ATCC 25922 and *Pseudomonas aeruginosa ATCC 27853*. Ceftriaxone and imipenem as positive controls were obtained from MAST Company.

In order to evaluate the antibiotic susceptibility of the compounds, agar disk diffusion method was used [28]. According to CLSI protocol, samples were placed in the Mueller–Hinton agar surface and then incubated at 35 °C. Finally, inhibition zone was measured for all tested compounds after 16–20 h. According to well-diffusion method, we made wells on the Mueller–Hinton agar surface using sterile Pasteur pipette and then 100 μL of the Ag-NPs solution and water was poured into the wells. After incubation at 37 °C for 16–20 h, the zone of inhibition was measured.

Results and Discussion

UV–Vis Spectra Analysis

One of the most interesting features of NPs is their optical properties. UV–Vis absorption spectroscopy is a useful technique to characterize the NPs synthesized. For metallic NPs, absorption wavelengths in the range of 300–800 nm are normally used for the characterization [29]. It has been demonstrated that Ag-NPs exhibit brownish colors originated from the excitation of surface plasmon resonance (SPR)

of the NPs [30]. This color strongly depends on the concentration and size of the Ag-NPs. However, typical Ag-NPs show maximum absorption peaks in the range of 400–500 nm [31]. UV–vis absorption spectrum of the Ag-NPs synthesized here using the extract of *Chelidonium majus* root, is depicted in Fig. 1. As it can be seen, characteristic absorption band of SP for 3.5 mM of the Ag NPs varies with increasing the interaction time, owing to increasing the production of Ag NPs which in turn resulted in the increase of absorption at 431 nm. On the other words, with the increase of reaction time, the SPR absorbance of the formed Ag nanoparticles gets stronger and the absorption value in λ_{max} rises from 0.64 to 1.46 indicating the formation of more Ag NPs. The reaction starts within 30 min when the SPR shows a detectable peak at 398 nm and ends after 24 h with an absorption peak at 431 nm. A 1-month-old sample also exhibits a peak at 431 nm.

X-ray Diffraction Analysis

Figure 2 shows the XRD analysis of the Ag NPs biosynthesized. The purity and size of the NPs were determined with X-ray diffraction using Kα radiation of Cu ($\lambda = 0.15406$ nm) in the angle range of 35°–80°. The XRD pattern confirms the crystalline structure of the NPs. In the spectrum, peaks observed at 38.1°, 44.3°, 64.5° and 77.4° are corresponded to (111), (200), (220) and (311) planes of pure silver confirming the successful biosynthesis of Ag-Nps. The average crystallite size of the biosynthesized Ag NPs has been estimated using Scherer formula [32, 33]:

$$D = 0.9\lambda/\beta Cos\theta$$

where D is the crystallite size, λ is the wavelength of the X-ray source (0.15406 nm), β is the

FWHM and θ is the angle of diffraction. According to the formula, average size of the Ag NPs has been calculated to be 21 nm. Some unassigned intense diffraction peaks are also observed in the spectrum which can be related to the crystallization of

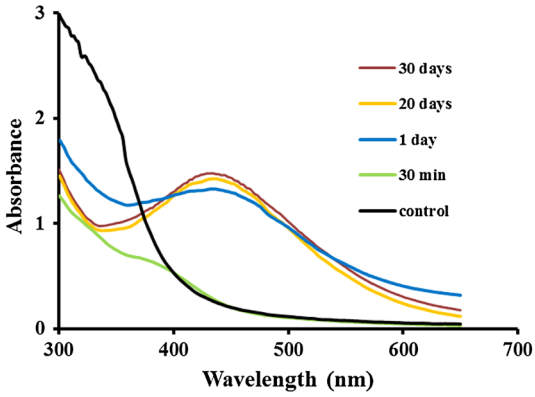

Fig. 1 Increase the Surface plasmon absorption of silver nanoparticles at different times (Color figure online)

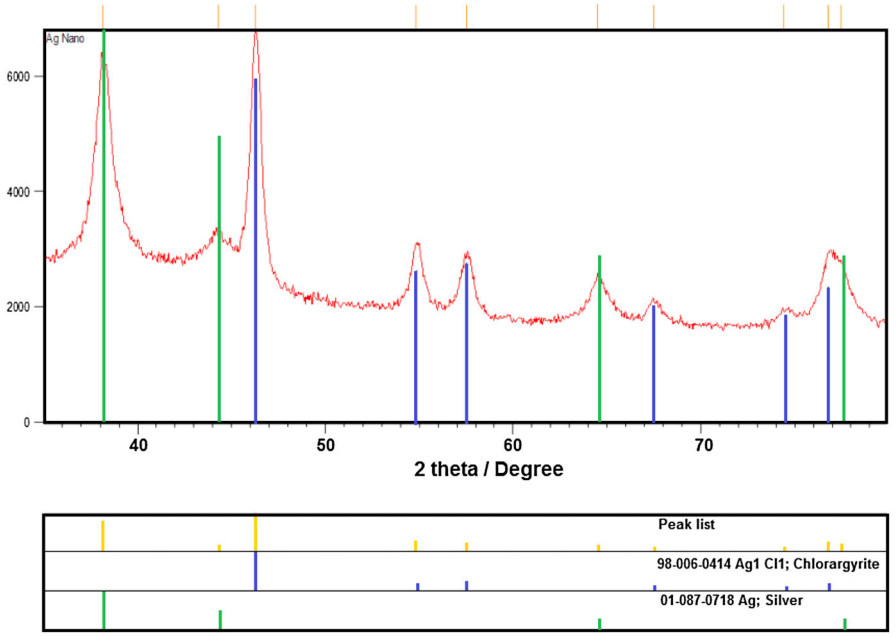

Fig. 2 The XRD patterns of silver nanoparticles synthesized (Color figure online)

bioorganic phases on the surface of the NPs. In addition, other crystallographic impurities such as AgCl are present in the XRD profile [34, 35]

Transmission Electron Microscopy (TEM) Analysis

Transmission electron microscopy (TEM) was also used for the determination of shape, average size and particle size distribution of the NPs. As it can be seen from Fig. 3, the synthesized particles are spherical. Also, particle size distribution analysis determined the average size of the NPs to be 15.42 nm (Fig. 4.) and approximately the synthesized Ag-NPs are homogeneous in nature.

Antibacterial Activity

Antimicrobial activities of the Ag-NPs against *Escherichia coli* which was isolated from clinical sample, *E. coli* -ATCC 25922 and *Pseudomonas aeruginosa* ATCC 27853 were assessed by evaluating the presence of inhibition zone (IZ). The inhibition zone pictograms are listed in Table 1. As shown in Fig. 5, the biosynthesized Ag-NPs could inhibit different pathogenic bacteria, including *P. aeruginosa* [35], and *E. coli* [36] previously reported. As it is clear from the results, the *E. coli* species isolated from the patients are sensitive to the Ag NPs at 150 and 300 ppm similar to the other tested species, *P. aeruginosa* and *E. coli*. Ag-NPs as

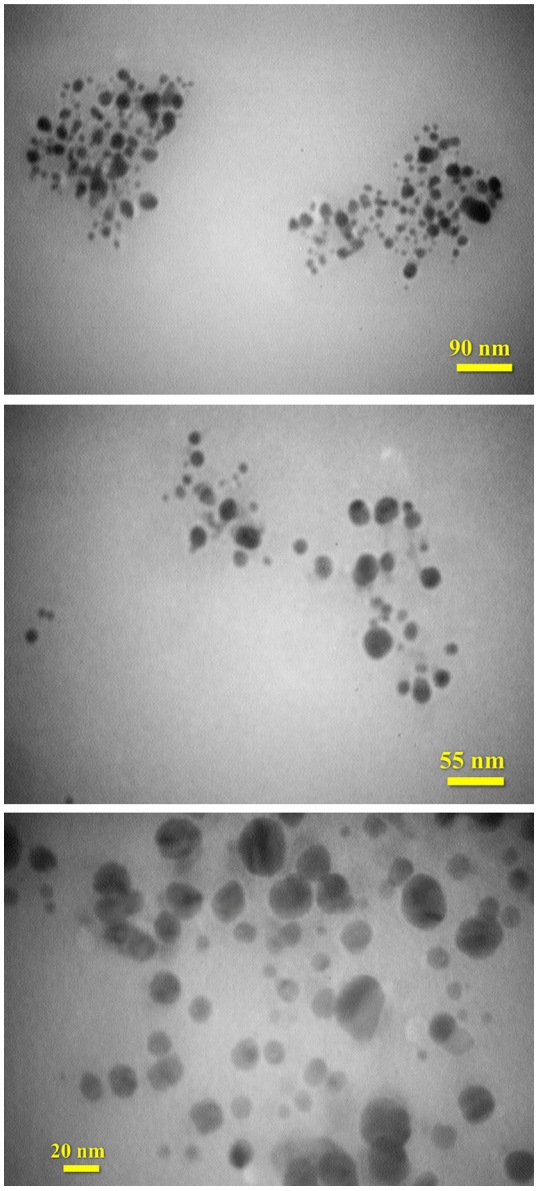

Fig. 3 TEM images of the Ag-NPs synthesized using the extract of *Chelidonium majus* root

well-known antibacterial agent have been demonstrated to act against bacteria with different mechanisms. Alteration of membrane permeability and respiration is the reported mechanism of the action of Ag-NPs against *E-coli* and *P. aeruginosa.* However another possible mechanism against the latter is irreversible damage on the bacterial cells [37].

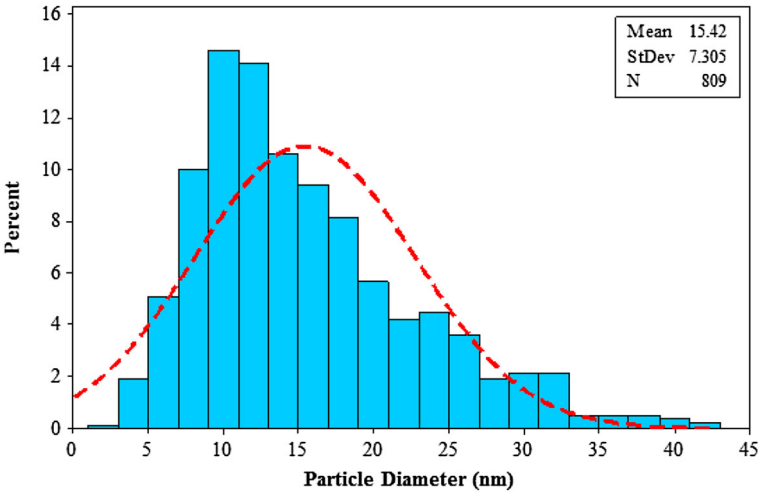

Fig. 4 Particle size distribution of the Ag-NPs

Table 1 Diameters of the inhibition zones corresponded to human pathogenic and standard strains after treating with different agents

Bacteria	Ag-Nps		Control negative	Control positive	
	150 ppm	300 ppm	Water	IMI	CTR
Inhibition zone(mm)					
E. coli ATCC 25922	12	12	NA	26	24
P. aeruginosa ATCC 27853	12	12	NA	26	26
E. coli	13	13	NA	25	24

NA not appeared, *IMI* imipenem, *CTR* Cefteriaxone

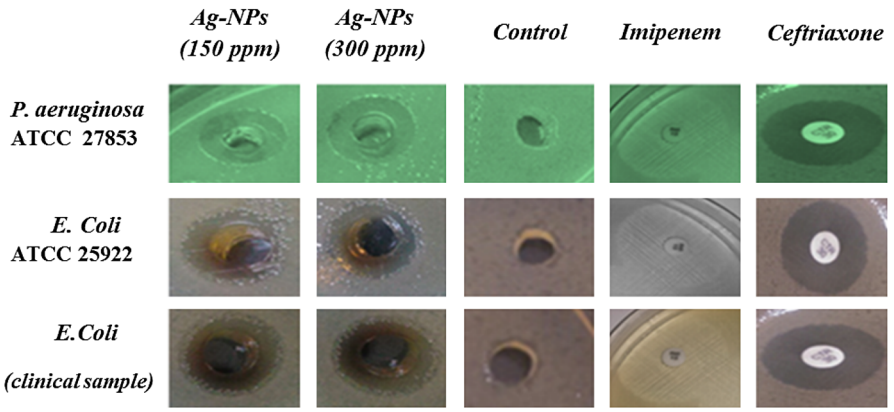

Fig. 5 Antibacterial activity of the biosynthesized Ag NPs against human pathogen and standard strains

Conclusion

We have developed a novel approach for the synthesis of silver nanoparticles which is green, low-cost, fast and simple compared with the other methods like physical and chemical synthesis of nanoparticles that consume high energy and hazardous chemicals. Extract of *chelidonium majus* root contains compounds which can act as reducing and capping agents for the synthesis of silver nanoparticles. The nanoparticles synthesized have been characterized to have mean diameter of 15.42 nm while the chemical and physical synthesized Ag-NPs has possesses a good significant antimicrobial effect against both Gram-positive and Gram-negative bacteria.

Acknowledgments Authors gratefully acknowledge the financial support provided for this work by the Shahid Bahonar University of Kerman

References

1. A. Mnyusiwalla, A. S. Daar, and P. A. Singer (2003). 'Mind the gap': science and ethics in nanotechnology. *Nanotechnology* **14**, R9.
2. C. B. Murray, C. Kagan, and M. Bawendi (2000). *Annu. Rev. Mater. Sci.* **30**, 545–610.
3. E. Hao, R. C. Bailey, G. C. Schatz, J. T. Hupp, and S. Li (2004). *Nano Lett.* **4**, 327–330.
4. M. J. Ahmed, G. Murtaza, A. Mehmood, and T. M. Bhatti (2015). *Mater. Lett.* **153**, 10–13.
5. A. E. Welles *Silver Nanoparticles: Properties* (Nova Science Publishers, Characterization and Applications, 2010).
6. K. M. A. El-Nour, A. A. Eftaiha, A. Al-Warthan, and R. A. Ammar (2010). *Arab. J. Chem.* **3**, 135–140.
7. C. Marambio-Jones and E. M. Hoek (2010). *J. Nanopart. Res.* **12**, 1531–1551.
8. A. K. Mittal, Y. Chisti, and U. C. Banerjee (2013). *Biotechnol. Adv.* **31**, 346–356.
9. J. Liu and G. Jiang *Silver nanoparticles in the environment* (Springer, Berlin, Heidelberg, 2015).
10. K. Shameli, M. B. Ahmad, W. Z. W. Yunus, N. A. Ibrahim, and M. Darroudi (2010). *Int. J. Nanomed.* **5**, 743–751.
11. A. Kutsenko and V. Granchak (2009). *Theor. Exp. Chem.* **45**, 313–318.
12. B. Yin, H. Ma, S. Wang, and S. Chen (2003). *J. Phys. Chem. B* **107**, 8898–8904.
13. S. Chen, T. Akai, K. Kadono, and T. Yazawa (2001). *Appl. Phys. Lett.* **79**, 3687–3689.
14. M. Darroudi, M. B. Ahmad, A. K. Zak, R. Zamiri, and M. Hakimi (2011). *Int. J. Mol. Sci.* **12**, 6346–6356.
15. X. Ye, Y. Zhou, J. Chen, and Y. Sun (2007). *Appl. Surf. Sci.* **253**, 6264–6267.
16. H. Yin, T. Yamamoto, Y. Wada, and S. Yanagida (2004). *Mater. Chem. Phys.* **83**, 66–70.
17. F. Mafuné, J.-Y. Kohno, Y. Takeda, T. Kondow, and H. Sawabe (2000). *J. Phys. Chem. B* **104**, 9111–9117.
18. E. Castro-Longoria, A. R. Vilchis-Nestor, and M. Avalos-Borja (2011). *Colloids Surf., B* **83**, 42–48.
19. R. Rajan, K. Chandran, S. L. Harper, S.-I. Yun, and P. T. Kalaichelvan (2015). *Ind. Crops Prod.* **70**, 356–373.
20. V. K. Sharma, R. A. Yngard, and Y. Lin (2009). *Adv. Colloid Interface Sci.* **145**, 83–96.
21. S. Iravani (2011). *Green Chem.* **13**, 2638–2650.
22. J. Huang, Q. Li, D. Sun, Y. Lu, Y. Su, X. Yang, H. Wang, Y. Wang, W. Shao, and N. He (2007). *Nanotechnology* **18**, 105104.
23. A. Saxena, R. Tripathi, F. Zafar, and P. Singh (2012). *Mater. Lett.* **67**, 91–94.
24. S. S. Shankar, A. Ahmad, and M. Sastry (2003). *Biotechnol. Progr.* **19**, 1627–1631.
25. N. Ahmad, S. Sharma, V. Singh, S. Shamsi, A. Fatma, and B. Mehta (2010). *Biotechnol. Res. Int.* **2011**, 1–8.
26. J. Kesharwani, K. Y. Yoon, J. Hwang, and M. Rai (2009). *J. Bionanosci.* **3**, 39–44.
27. D. M. Ledwith, A. M. Whelan, and J. M. Kelly (2007). *J. Mater. Chem.* **17**, 2459–2464.

28. R. Schwalbe, L. Steele-Moore, and A. C. Goodwin *Antimicrobial susceptibility testing protocols* (CRC Press, Boca Raton, 2007).
29. C. S. S. R. Kumar *UV-VIS and photoluminescence spectroscopy for nanomaterials characterization* (Springer, Berlin, 2013).
30. P. Mulvaney (1996). *Langmuir* **12**, 788–800.
31. F. Cheng, J. W. Betts, S. M. Kelly, and A. L. Hector (2015). *Mater. Sci. Eng. C* **46**, 530–537.
32. A. Patterson (1939). *Phys. Rev.* **56**, 978–982.
33. S. Y. Ebrahimipour, I. Sheikhshoaie, J. Castro, W. Haase, M. Mohamadi, S. Foro, M. Sheikhshoaie, and S. Esmaeili-Mahani (2015). *Inorg. Chim. Acta* **430**, 245–252.
34. S. Ashokkumar, S. Ravi, V. Kathiravan, and S. Velmurugan (2015). *Spectrochim. Acta, Part A* **134**, 34–39.
35. A. Miri, M. Sarani, M. R. Bazaz, and M. Darroudi (2015). *Spectrochim. Acta, Part A* **141**, 287–291.
36. M. E. Barbinta-Patrascu, C. Ungureanu, S. M. Iordache, I. R. Bunghez, N. Badea, and I. Rau (2014). *J. Mater. Chem. B* **2**, 3221–3231.
37. G. Franci, A. Falanga, S. Galdiero, L. Palomba, M. Rai, G. Morelli, and M. Galdiero (2015). *Molecules* **20**, (5), 8856–8874.